A comparison of line-sources of buoyancy placed near and far from a wall

David Parker*[1], Henry Burridge[2], Jamie Partridge[1] and Paul Linden[1]

1 Department of Applied Mathematics and Theoretical Physics, University of Cambridge, Centre for Mathematical Sciences Wilberforce Road, Cambridge CB3 0WA, UK
**Corresponding author: dap58@cam.ac.uk*

2 Department of Civil Engineering and Environmental Engineering, Imperial College London, London, SW7 2AZ, UK

ABSTRACT

Experiments are presented on turbulent buoyant free-line and wall plumes, whereby the buoyancy source is emitted from a horizontal line source, in one case free of the presence of a wall and in the other placed immediately adjacent to a wall. The dynamics of turbulent entrainment, whereby ambient fluid is mixed in to the plume, are explored. The velocity field and scalar edge of the plumes are measured. From this the time-averaged plume-width and volume flux are compared. The spreading rate, and therefore the entrainment, of the wall plume is found to be half that of the free-line plume, indicating that the wall has a significant effect on the entrainment process. Further, the volume flux of the wall plume is found to be half that of the free-line plume, indicating that larger maximum scalar concentrations are present in the wall plume. The effect that the reduced entrainment rate has on a typical heated room, via a line source of buoyancy, is demonstrated by comparing a numerical model of the developing temperature stratification within a sealed enclosure in the case of the line source near a wall and away from a wall, where in particular it is found that higher maximum temperatures are present for the case of the line source near a wall.

KEYWORDS

Turbulent Convection, Plumes, Ventilation

INTRODUCTION

Flows driven by line sources of buoyancy often appear within buildings, for example in the case of heating, from radiators, or cooling, from chilled beams. The process of turbulent entrainment in these flows is key to understanding how they evolve and how one might model them. It has been observed that the entrainment is reduced when a line source of buoyancy is positioned immediately adjacent to a wall (Sangras et al. (2000), Grella & Faeth (1975)) and reduced further when the source is vertically distributed along a wall (Cooper & Hunt (2010), McChonnochie & Kerr (2015)). Partly due to the lack of understanding of this effect there remain unanswered fundamental questions regarding the thermal stratification that results from distributed sources placed on the wall within both sealed and ventilated spaces. In order to isolate the effect a wall has on the entrainment process it is instructive to compare two buoyancy driven flows that differ only by the presence of a wall. In our case, this is done comparing line plumes, in the absence of any boundary, and wall plumes, when the line source is adjacent to a vertical boundary. These flows are the obvious choice for this type of study since a vertically distributed buoyancy source without the presence of a wall is not easily achieved.

The study of line plumes has received more recent attention than wall plumes, in particular the work of Paillat & Kaminski (2014) which we outline briefly in the following section. In §2 we introduce the theory and present a review of previous work on free-line and wall plumes. In §3 velocity field and scalar edge data of free-line plumes and wall plumes are presented.
The data are compared between the two flows and implications for entrainment are considered. In particular, it is shown how the reduced entrainment due to the wall will affect the developing stratification within a sealed room.

THEORY AND PREVIOUS WORK

A free-line plume is created from a continuous source of buoyancy released from a horizontal line. A wall plume is created from a continuous source of buoyancy released from a horizontal line which is placed immediately adjacent to an adiabatic wall. Figure 1 shows a simplified diagram of a time-averaged free-line and wall plume.

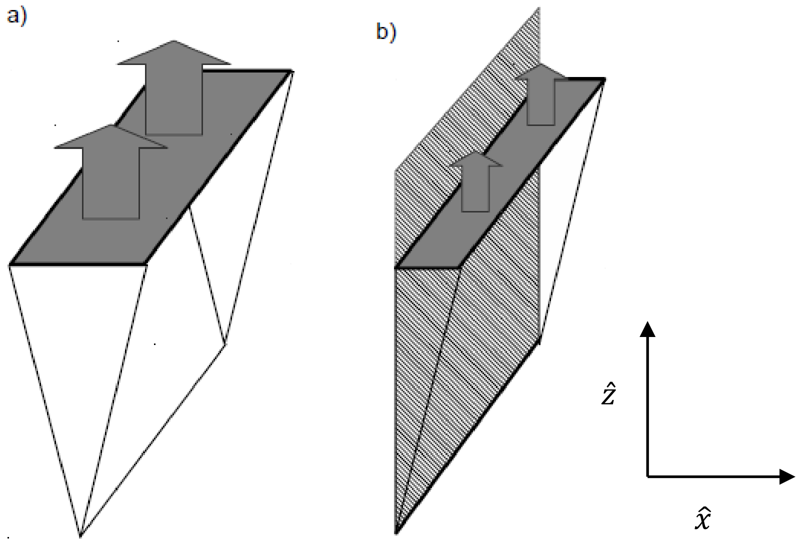

Figure 1: Time-averaged diagram of a free-line plume and a b) wall plume within an environment of constant density.

The fluxes of volume, Q, momentum, M , and buoyancy, F , in the plume per unit width for a free-line plume may be written as follows

$$Q = \int_{-\infty}^{\infty} w dx\,, \qquad M = \int_{-\infty}^{\infty} w dx\,, \qquad F = \int_{-\infty}^{\infty} g \frac{\rho - \rho_a}{\rho_a} w\, dx, \tag{1}$$

where $\rho(z)$ and $\rho_a(z)$ are the density of the plume and ambient respectively. For a wall plume they may be written

$$Q = \int_{0}^{\infty} w dx\,, \qquad M = \int_{0}^{\infty} w dx\,, \qquad F = \int_{0}^{\infty} g \frac{\rho - \rho_a}{\rho_a} w\, dx, \tag{2}$$

For a free-line plume the conservation of volume, momentum and buoyancy flux may be written as follows, (Paillat & Kaminski 2014)

$$\frac{dQ}{dz} = 2\alpha_f \frac{M}{Q}\,, \quad \frac{dM}{dz} = \int_{-\infty}^{\infty} g \frac{\rho - \rho_a}{\rho_a} dx, \qquad \frac{dF}{dz} = 0, \tag{3}$$

where α_f is the entrainment coefficient for the free-line plume and for a wall plume the equivalent expressions may be written

$$\frac{dQ}{dz} = \alpha_w \frac{M}{Q}\ , \qquad \frac{dM}{dz} = \int_0^\infty g\frac{\rho-\rho_a}{\rho_a}dx - \epsilon, \qquad \frac{dF}{dz} = 0, \tag{4}$$

Where α_w is the entrainment coefficient for the wall plume and ϵ is the wall shear stress. Grella & Faeth (1975) find that the wall shear stress is not large compared to the buoyancy force, so we will assume it is negligible in our study. It should be noted, however, that the shear stress does not enter the volume flux balance and so does not affect one of the main purposes of the study, to determine the entrainment coefficient.

We note that in the formulations of (3) and (4) there is no assumption on the shape of the velocity and buoyancy profiles, so it is useful to consider the plume equations in this form since the velocity and buoyancy profiles of the two flows will naturally be different. Self-similarity is found in all studies that measure the velocity and buoyancy profiles in both the free-line and wall plume. In particular, Grella & Faeth (1975) define

$$\frac{\overline{w}}{\overline{w}_m} = W\left(\frac{x}{x-z_o}\right), \qquad \frac{\overline{g'}}{\overline{g'_m}} = G'\left(\frac{x}{x-z_o}\right), \tag{5}$$

where $g' = g\frac{\rho-\rho_a}{\rho_a}$, W and G' are universal functions far from the source, z_o is the virtual origin and the overline indicates time-averaged data. For the free-line plume the functions are approximated very well by a Gaussian. The wall plume profiles are more complex due to the lack of symmetry. By assuming power law solutions for Q, M and F the relations $dQ^2/dz = 2\alpha$ and $dQ^2/dz = \alpha$ may be derived for the free-line and wall plume, respectively (Paillat & Kaminski 2014).

By assuming the velocity and buoyancy profiles are Gaussian, Paillat & Kaminski (2014) provide a theoretical framework of entrainment in free-line plumes and determine an expression for the entrainment value depending only on the ratio of the widths of buoyancy and velocity profiles and the self-similar Reynolds stress profile. This is compared to an experimentally determined entrainment coefficient, α_g , based on the Gaussian width of the time-averaged plume, b_w , and is defined by $db_w/dz = 2\alpha_g$ which may be related to α by $\alpha\ = \sqrt{2\pi}\alpha_g$ assuming the Gaussian profiles. Good agreement is found between the experimentally determined α_g and the model. Ramaprian & Chandrasekhara (1989) focus instead on the entrainment relation $\alpha_m = \frac{1}{w_m}\ dQ/dz$, which makes no assumption of a Gaussian profile but, if imposed, the relation $\alpha\ =\ \sqrt{2}\alpha_m$ may be derived. Most studies on wall plumes also focus on α_m , although in some cases α was also calculated. Since the velocity profile of the wall plume is not a known analytic function, a theoretical relation between α_m and α has not been derived, however, Grella & Faeth (1975) find that $\alpha/\alpha_m = 1.43 \approx 2$. Details of the experiments in previous studies for both free-line and wall plumes are shown in table 1.

Table 1: Experimental data of previous studies of free-line and wall plume. [1] Sangras et al. (2000), [2] Lai & Faeth (1987), [3] Grella & Faeth (1975), [4] Ramaprian & Chandrasekhara (1989), [5] Paillat & Kaminski (2014). * It is not clear how the average velocity in the plume was calculated for this study and it may differ from the other studies where M/Q is used.**Explicit α was not calculated but the relation $\alpha\ = \sqrt{2\pi}\alpha_g$ has been used. A dash is placed where data were not made available.

	[1]	[2]	[3]	[4]	[5]
Plume Type	Wall	Wall	Wall	Free	Free
Experiment	Helium and air	C02 and air	Heated air	Heated water	Ethanol and water
α_m	0.068	0.071*	0.067	0.11	-

α	-	0.17	0.095	0.158	0.165**

For the wall plume data presented in the table, the buoyancy flux is that associated with an equivalent free-line plume so that a direct comparison between velocities may be made. From table 1 the studies on wall plumes agree that the entrainment coefficient, α_m , has a value of 0.069 ± 0.02. It is also clear that the studies of free-line plumes agree relatively well on the entrainment coefficient, α, with a value $\alpha = 0.16$. It should be noted that Lai & Faeth (1987) calculate the average velocity, $\overline{w}_a$, used in the calculation of α, by the relation

$$\overline{w}_a = \frac{1}{\delta}\int_0^{\delta} \overline{w} dx \tag{6}$$

where δ is some boundary layer thickness, which is not defined. Therefore, it is not clear, especially given the relatively high value, whether their calculation is equivalent to the top-hat velocity M/Q used in the other studies. Given that the two flows will have different velocity profiles it seems natural to compare the entrainment rates using the bulk flow properties and not the maximum velocity, i.e. a comparison of α and not α_m. It is therefore unfortunate that for the wall plume case less attention has been given to this entrainment coefficient and there is not good consensus about the value. As well as the studies presented in table 1 there have been four other notable previous studies on free-line plumes for which data is presented in Van Den Bremer & Hunt (2014) and entrainment coefficients reported are in the range $\alpha = [0.14, 0.23]$.
A broad finding among the studies of Grella & Faeth (1975), Lai & Faeth (1987) and Sangras et al. (2000) is an entrainment coefficient, based on the maximum vertical velocity, in the wall plume approximately half that of the free-line case. They largely attribute this reduction in the entrainment coefficient to the wall preventing mixing by inhibiting the meandering motion of the plume centreline which reduces the length scale of the large-scale structures. However, little more is said about the large-scale dynamics beyond this. Given that, at least for an axisymmetric plume, where it is thought that the large-scale structures, in the form of eddies, forming at the edge of the plume are necessary for turbulent entrainment it would be illuminating to study, in more detail, the effect of the wall on these large-scale structures.

EXPERIMENTS

To study the difference in turbulent entrainment between free-line and wall plumes experiments were designed to generate the two flows. The experiments were performed in a tank of horizontal cross-section 100 cm x 80 cm filled with dilute saline solution (of uniform density ρ_a) to a depth of 80 cm. Relatively dense source fluid, Sodium Nitrate solution, was supplied to a line source nozzle of width b = 0.1 cm for the free-line plume and b = 0.05 cm for the wall plume and length 15 cm in both cases. The use of Sodium Nitrate allowed for a refractive index match between the ambient and source fluid. This was necessary so that position of the PIV particles were not distorted by refractive index changes. The flow was enclosed by two walls perpendicular to the source, separated by the length of the source, of dimension 60 cm x 60 cm to promote the two dimensionality of the flow. PIV was performed with seeded particles of diameter 50μm. Videos of the experiments were recorded at a frame rate of 50 Hz with 8000 frames for each individual experiment. Details of the experimental parameters are given in table 2. For both the free-line and wall plume case the data was checked for self-similarity by the independence of maximum vertical velocity with height.

Velocity profiles for distances greater than 150b from the source were used and found to be self-similar, in agreement with Paillat & Kaminski (2014). However, we found that a larger distance than 150b was required, which is not surprising given our smaller source Reynolds number. Sangras et al. (2000) suggest a distance greater than 92b for wall plumes, however they have a significantly higher source Reynolds number because they are using Helium and air for the experiment. It is well established that wall plumes require a greater source distance than for free-line plumes to reach self-similarity, so given our Reynolds number is the same order as Paillat & Kaminski (2014) we expect a distance greater than 150b. For the free-line plume data presented from our study no attempt was made to create a pure plume, $Ri_0 \approx .14$ (Paillat & Kaminski 2014), at the source. Paillat & Kaminski (2014) and Ramaprian & Chandrasekhara (1989) used only a relatively forced plume, $Ri_0 = 0.005 - 0.07$, but using buoyancy field measurements it was found that the plume adjusts to a pure plume in the region of self-similarity. An independent set of experiments were also performed where fluorescein was added to the source fluid for the wall plume and free-line plume. This was purely done to perform analysis on the statistics of the position of the scalar edge of the plume and no attempt was made to infer any buoyancy field data from the images. Test conditions for these experiments were the same, to within experimental uncertainty, as the PIV experiments 1 for the free-line plume and wall plume shown in table 2, therefore we can be confident the plumes are self-similar.

RESULTS

A virtual origin, z_o, was first determined for each set of data by assuming a linear growth rate of the plume width and where our measurements imply $R(z_o) = 0$, where R is defined for each flow by (7). Using this correction self-similarity was found in both cases by the scalings in equations (5) for the vertical and horizontal velocities, figure 2 c). In order to directly compare velocity profiles, we non-dimensionalise data for both flows using the physical buoyancy flux, F, of that associated with wall plume. Profile shapes of the free-line plume agree well with Paillat & Kaminski (2014) and those of the wall plume case agree well with Sangras et al. (2000). Integration of the velocity profiles shows that for a given buoyancy flux, F, the volume flux, Q, of a wall plume is half that of a free-line plume. This is a consequence of the wall preventing mixing of the wall plume. From the definition of F it is clear that if the volume flux is reduced, for the same buoyancy flux, then the wall plume must have higher scalar concentrations within the plume. The effect this will have on the stratification of an enclosed room is shown in the next section.
To aid comparison between the flows we define the plume half-widths as

$$\bar{R} = \begin{cases} \dfrac{1}{2}\dfrac{\bar{Q}^2}{\bar{M}} & \text{for the free} - \text{line plume}, \\ \dfrac{\bar{Q}^2}{\bar{M}} & \text{for the wall plume}. \end{cases} \tag{7}$$

These may be interpreted as the top-hat plume half-width for the free-line plume and the total width of the flow for the wall plume. The plume widths for all the experiments are shown in figure 3. The data for each flow broadly fit a linear growth rate where, as expected, a lower growth rate is observed in the wall plume. The entrainment coefficients were calculated using this data and were found to be $\alpha = 0.08 \pm 0.01$ for the wall plume and $\alpha = 0.15 \pm 0.01$ for the free-line plume. This broadly matches with previous experiments, table 1. The maximum wall plume velocities are on average greater than for the free-line plume by 5%. This is due to the increased buoyancy close to the wall which is unable to be mixed as effectively as the free-line case (Sangras et al. 2000). Two typical images of the plumes, taken from the experiments where fluorescein was added to the plume fluid, are shown in figure 2. The typical meandering motion of the free-line plume, 2 b), is visible. There are very large regions of ambient fluid between pockets of plume fluid, which can be seen at the top of the image.

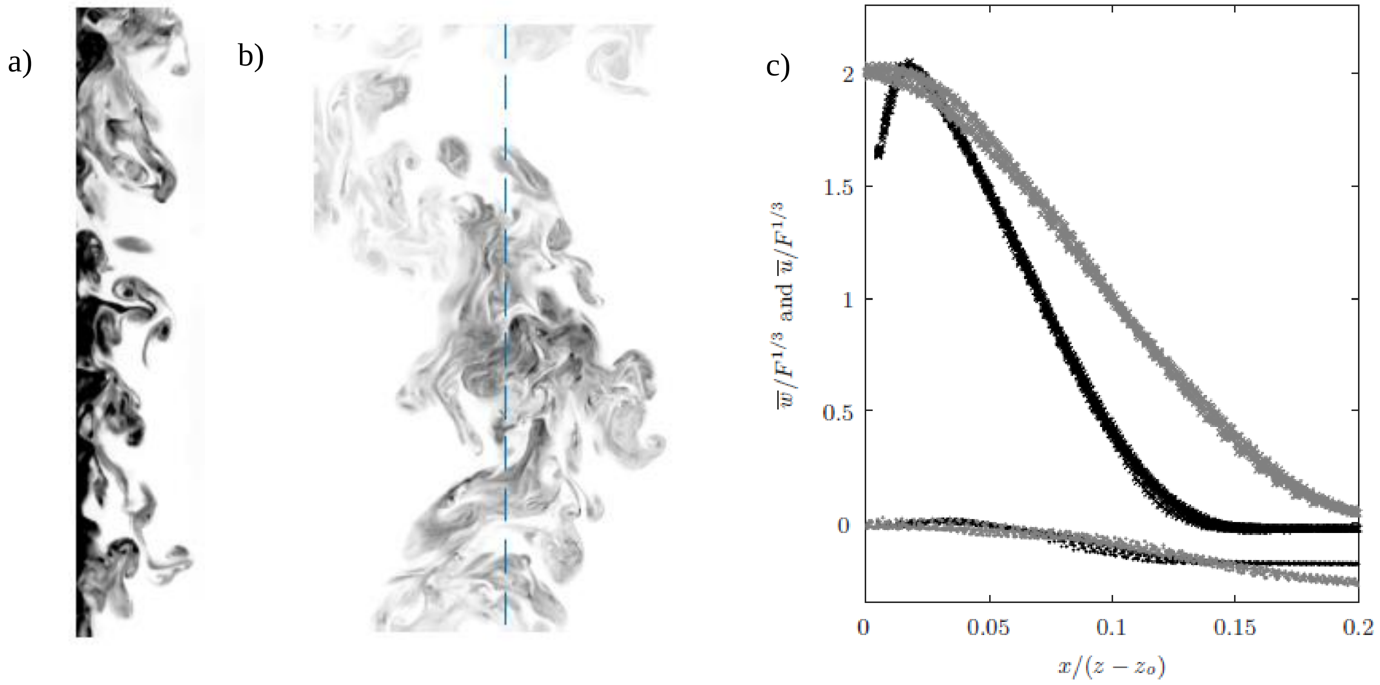

Figure 2: A snapshot of the experiment for a) a wall plume and b) free-line plume. The blue dashed line indicates the position of the source. c) Vertical, crosses, and horizontal, dots, velocity data for free-line, grey, and wall plume, black. Data from experiments 1 are used in both cases and 20 heights are plotted spanning the whole height. For the wall plume case the velocities are scaled using double the physical buoyancy flux in order to make a direct comparison of the velocities.

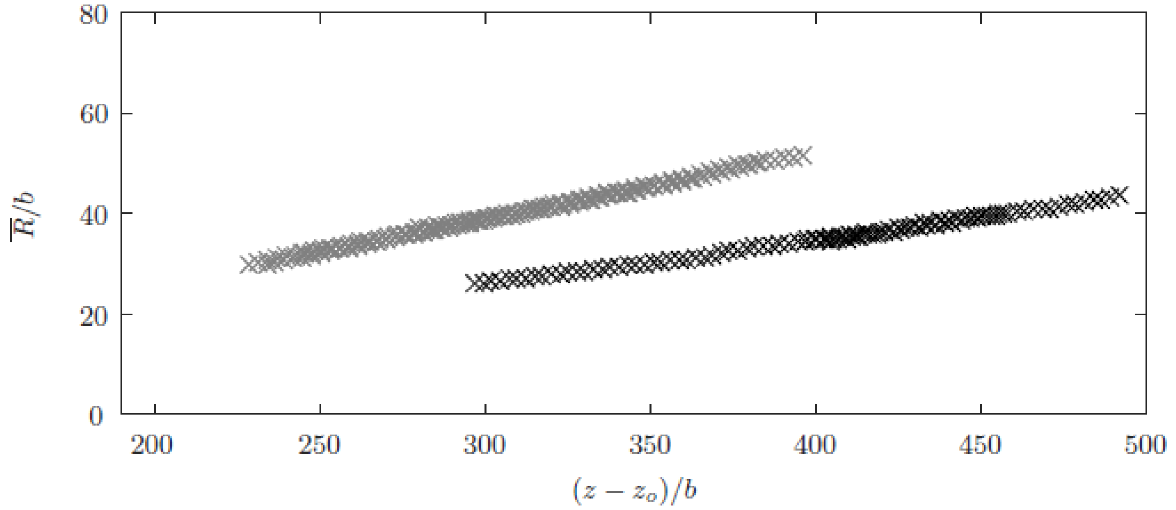

Figure 3: Mean plume widths as defined in (7) for free-line plumes, grey, and wall plumes, black. Both the free-line and wall plume data are scaled on the free-line source width, b.

At times, ambient fluid is completely transported from one side of the plume to the other, a behaviour which is not typically seen in an axisymmetric plume. Meandering of the scalar edge is also seen in the wall plume. Regions of ambient fluid may be found very close to the wall, again between pockets of plume fluid. The time-averaged position of the scalar edges of the plumes were calculated from the experiments where fluorescein was added to the plume. This was done by using a Canny edge-detection algorithm (Canny 1986) on each snapshot and finding the outer edge of plume.

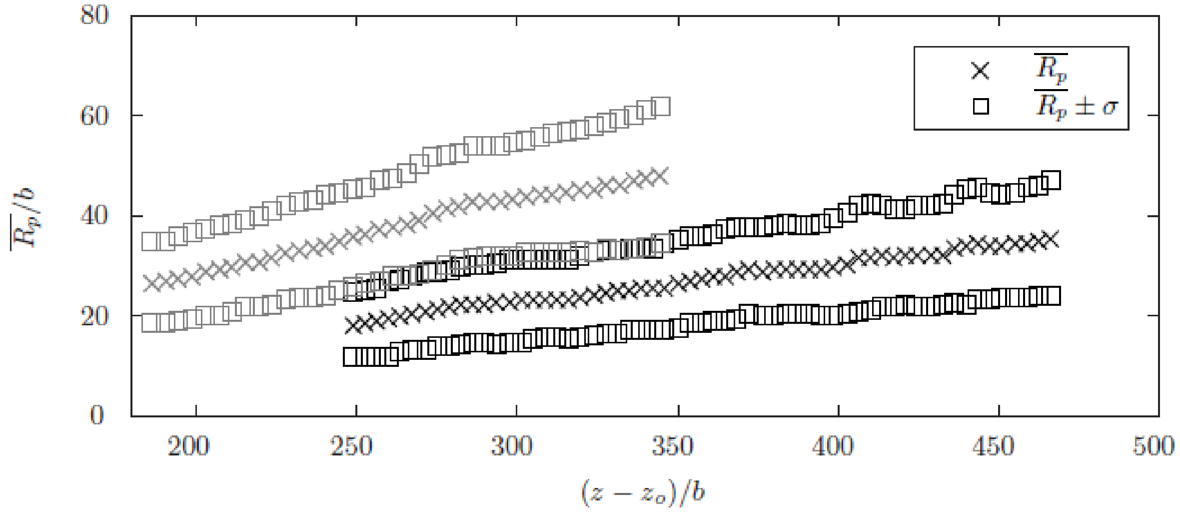

Figure 4: Mean scalar plume widths $\overline{R_p}$, crosses, and the variation in scalar plume widths $R_p \pm \sigma$, squares, for free-line plumes, grey, and wall plumes, black. Both the free-line and wall plume data are scaled on the free-line source width, b.

For the free-line plume we define the scalar width, R_p, as half the distance between the right edge and the left edge of the plume. For the wall plume we define the scalar width as the distance of the outer scalar edge to the wall. The time-averaged position and variation of the plume scalar edge are shown in figure 4. They broadly exhibit linear growth rates with height.

Table 2: Plume experimental data of free line plumes (1F, 2F and 3F) and wall plumes (1W, 2W and 3W)

Parameter	**Definition**	**1F**	**2F**	**3F**	**1W**	**2W**	**3W**
Buoyancy Flux	$F_0 = Q_0 g'$	13.6	18.1	14.7	10.4	10.4	10.4
Source Richardson number	$Ri_0 = F_0 Q_0^3 / M_0^3$	0.045	0.0097	0.014	0.0206	0.0206	0.0286
Source Reynolds number	$Re_0 = Q_0/\nu$	67	123	103	50	50	42
Characteristic plume Reynolds number	$\bar{w}_m \bar{R}/\nu$	2900-5200	3080-4650	2900-45900	1470-2070	2000-2350	2000-2500
α_m	$\frac{1}{\bar{w}_m} d\bar{Q}/dz$	0.094	0.093	0.090	0.068	0.062	0.063
α	$d\bar{R}/dz$	0.156	0.163	0.145	0.087	0.086	0.066
W_{max}	$\bar{w}_m / F^{1/3}$	2.04	1.90	2.00	2.05	2.12	2.07

APPLICATION TO HEATED ROOM

We have shown that the volume flux within a wall plume is significantly reduced and as a consequence, scalar concentrations within the wall plume will be greater than for a free-line plume. We set this in context with a heated room where we compare the developing stratification resulting from a line heat source, with the same heat flux, next to a wall and away from the wall within a sealed enclosure. We use the model of Baines and Turner (1969) where the plume develops according to the following equations

$$\frac{dQ}{dz} = \alpha\frac{M}{Q}, \qquad \frac{dM}{dz} = \frac{FQ}{M}, \qquad \frac{dF}{dz} = Q\frac{\partial\Delta_a}{\partial z}, \tag{8}$$

where $\Delta_a = g\beta\Delta T$ is the ambient buoyancy field. Which is assumed to follow an advection model

$$\frac{\partial\Delta_a}{\partial t} = \frac{Q}{L}\frac{\partial\Delta_a}{\partial z}, \tag{9}$$

where L is the width of the room. Initially, it is assumed that the ambient has $\Delta_a = 0$ everywhere. After each time step, a layer is formed at the top of the enclosure such that the density is given by that in plume at that height. The thickness of the layer is determined by Q at that height. The layers are advected down according to (9).

We take a typical room of dimension $H \times L = 4 \times 4m$, and a heat source of $100W/m$ with initial temperature $18°C$. Figure 5 shows the resulting ambient temperature profiles for different times for both flows. It can be see that, for a given time, the maximum temperatures for the wall plume are higher and the falling temperature interface descends at a slower rate. This may be desirable in the case of pollutants that passively trace buoyant fluid. For example, the exit vent may be at the top of the room so as little mixing as possible before the ceiling is reached is desirable. On the other hand, if the sole purpose of the line source is to heat the room then it's more likely a more well-mixed room would be desirable.

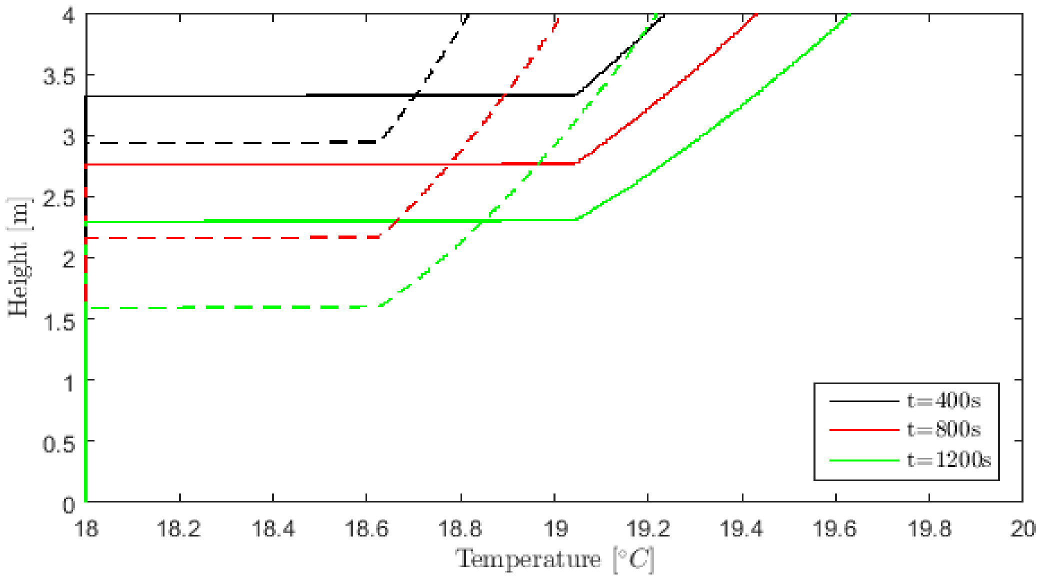

Figure 5: Evolution of the ambient temperature stratification profiles of free-line plume (dashed lines) and wall plumes (solid lines) for times t=400s (Black), t=800s (Red) and t=1200s (Green).

CONCLUSIONS

In this experimental study of line plumes and wall plumes we have observed the effects that an adiabatic wall has on a line source, which is placed immediately adjacent to it. We have found, in agreement with Sangras et al. (2000) and Grella & Faeth (1975), that the entrainment is significantly reduced and that $\alpha_f/\alpha_w = 2$. The velocity profiles of the two flows are presented and compared from which it is found that the spreading rate and volume flux in the wall plume is half that of the free-line plume, for a given buoyancy flux and distance from the source. From this we can conclude that scalar concentrations within the wall plume are greater than for a line plume, due to the wall preventing mixing with the ambient environment. We show, via a numerical model of a line heat source within an enclosed environment, how the temperature stratification would vary according to whether the line heat source is placed near or far away from a wall. As expected, larger maximum temperatures are found in the case of the heat source near a wall which may or may not be advantageous deepening on the application of the source.

REFERENCES

Baines, W. D. & Turner, J. S. (1969) *Turbulent buoyant convection from a source in a confined region*. Journal of Fluid Mechanics 37, 51–80.

Canny, J. (1986) *A computational approach to edge detection*. IEEE Transactions on Pattern Analysis and Machine Intelligence 646, 679–698.

Cooper, P. & Hunt, G.R. (2010) *The ventilated filling box containing a vertically distributed source of buoyancy.* Journal of Fluid Mechanics 646, 39–58.

Grella, J. J. & Faeth, G. M. (*1975) Measurements in a two-dimensional thermal plume along a vertical adiabatic wall.* Journal of Fluid Mechanics 71, 701–710.

Lai, M.-C. & Faeth, G.M. (1987) *Turbulent structures of adiabatic wall plumes.* Journal of Heat Transfer 109 (3), 663–670.

McConnochie, C.D. & Kerr, R.C. (*2015) The turbulent wall plume from a vertically distributed source of buoyancy*. Journal of Fluid Mechanics 787, 237–253.

Morton, B. R., Taylor, G. I. & Turner, J. S. (1956) *Turbulent gravitational convection from maintained and instantaneous sources.* Proc. R. Soc. Lond. 234, 1–24.

Paillat, S. & Kaminski, E. (2014) *Entrainment in plane turbulent pure plumes.* Journal of Fluid Mechanics 755, R2.

Ramaprian, B. R. & Chandrasekhara, M. S. (1989) *Measurements in Vertical Plane Turbulent Plumes.* Journal of Fluids Engineering 111, 69–77.

Sangras, R., Dai, Z. & Faeth, G.M. (2000) *Velocity statistics of plane self-preserving buoyant turbulent adiabatic wall plumes.* Journal of Heat Transfer 122 (4), 693–700.

Van Den Bremer, T. S. & Hunt, G.R. (2014) *Two-dimensional planar plumes and fountains.* Journal of Fluid Mechanics 750, 210–244.